

OBSERVATIONS OF COSMIC-RAY PRIMARIES IN THE ENERGY REGION
 $10^{12} \sim 10^{14}$ eV/particleY.Kawamura, H.Matsutani, H.Nanjyo, M.Saito, K.Teraoka, K.Toda, Z.Watanabe
Department of Physics, Hirosaki University, Hirosaki, JapanM.Ichimura, E.Kamioka, K.Kiriii, T.Kobayashi, T.Shibata, K.Shibuta, Y.Yoshizumi
Department of Physics, Aoyama Gakuin University, Tokyo, JapanH.Sugimoto
Sagami Institute of Technology, Fujisawa, Kanagawa, JapanK.Nakazawa
Physics Department, Gifu University, Gifu, Japan

Abstract

We have performed several balloon-borne experiments at Sanriku Balloon Flight Center in Japan. We report here these experimental results, particularly those obtained with use of screen-type X-ray film in 1988, and compare them with those of other groups. We found an indication that iron primary becomes significant at energies $\sim 10^{14}$ eV/nucleus, and seems to be comparable with the proton flux somewhere between 10^{13} and 10^{14} eV/nucleus.

Introduction Since 1987, we have continued to observe primary cosmic-rays with use of balloon-borne emulsion chamber at Sanriku, Japan. The purpose of our project is to confirm definitely the chemical composition and energy spectra of primaries in the energy region $10^{12} \sim 10^{14}$ eV/particle. In table 1, we summarize the situation of past three experiments, among which the results of the first one, '87-chamber, were reported in detail most recently in ref. 1. In the present paper, we report the results of '88-chamber, somewhat different type from orthodox emulsion calorimeter chamber, and compare them with those of '87-chamber.

CH.No.	Launch date	Exposure time	Chamber area	Altitude
1	1987/May/25	11.18×10^4 sec	4.00×10^3 cm ²	32.8 g/cm ²
2	1988/May/28	7.09×10^4	3.05×10^3	19.4
3	1989/May/25	6.96×10^4	15.50×10^3	11.7

Table 1. Flight situation of our balloon-borne emulsion chamber experiment.

Preliminary results of '89-chamber, a new type of chamber without calorimeter part, were presented in OG 6.1-6 of this volume, and the technical detail of our new type of chamber is reported in OG 10.5-1.

Flight situation and chamber structure

The balloon was launched in 1988/May/28 from Sanriku Balloon Flight Center, Institute of Space and Astronautical Science (Sagamihara, Japan), and recovered successively off Sakai in the Sea of Japan. In fig. 1, we present flight record.

The chamber structure is illustrat-

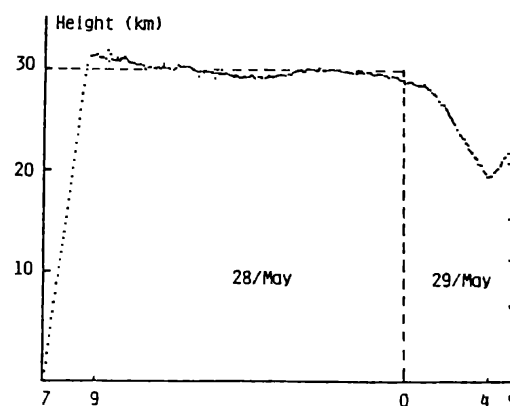
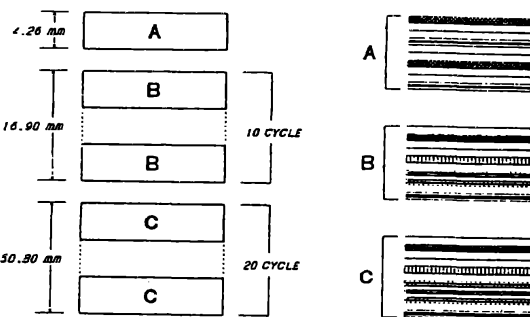


Fig. 1. Flight record of '88-chamber.

ed in fig. 2. While the chamber structure of '87-experiment was of orthodox type with use of #200-type X-ray film (non-screen type), the present one consists of essentially multi-layered screen-type X-ray film (hereafter called SXF, or HR-H film), details of which are presented in OG 10.5-1. The area of chamber is 3050 cm², and the thickness is 13.7 cm, corresponding to 0.892 collision m.f.p. for iron component.



Tracing and energy determination Detection of electromagnetic cascade shower is performed with use of both X-ray films, non-screen type (Fuji #200) and screen type (Fuji Grenex + HR-H X-ray film). We detected 188 showers from the former, while 556 from the latter. Vertex point of nuclear interaction, origin of each shower, is found by two methods, one from an orthodox way tracing back each shower with use of overlaid nuclear emulsion plates, and the other from direct detection with use of SXF, well possible by naked eye for high multiplicity, say more than ~ 50 , which makes us quite efficient to accumulate nuclear interaction events.

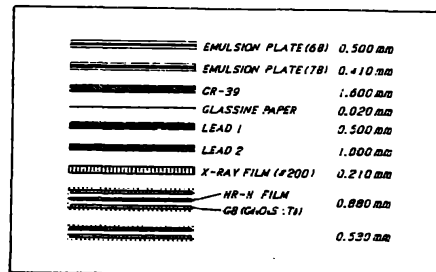


Fig. 2. '88-chamber structure

The energy determination with use of #200-type X-ray film has been often reported,^{1, 4, 5} so we present shortly its procedure in the case of SXF only. In fig. 3, we show an example of transition of spot darkness recorded on both X-ray films, SXF (open circle) and #200 (black circle), where the shower energy is 8.3 TeV with zenith angle of 67.6°. Since the peak of transition curve of spot darkness corresponds straightforwardly to the shower energy, in fig. 4 we compare each transition maximum D_{max} with shower energy obtained by electron-track-counting method with use of nuclear emulsion plate. The guiding curves drawn there are obtained by simulation calculation in the case of #200-type, while expected from optical characteristic of HR-H film itself in the case of SXF.

In fig. 5, we present the relation between both energies obtained by #200-type and SXF, well consistent with each other.

In fig. 6, we show differential energy spectrum of ΣE_γ thus obtained, which are drawn irrespectively of kind of primary charge in order to check the reliability of energy estimation in the lower energy region obtained

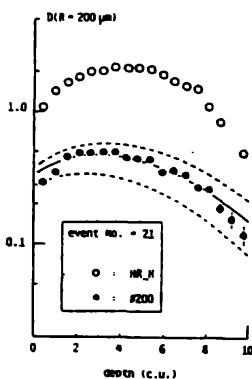


Fig. 3. Example of transition curve.

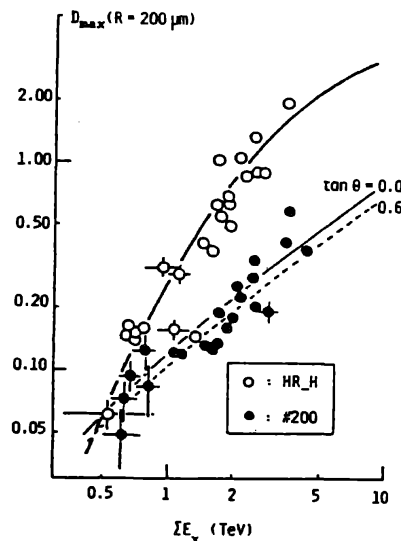


Fig. 4. Energy calibration of maximum spot darkness.

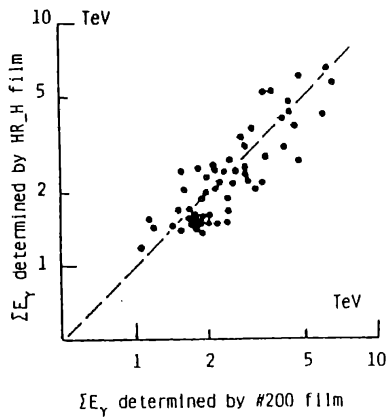


Fig. 5. Correlation between ΣE_{γ} obtained by #200-type X-ray film and that by SXF.

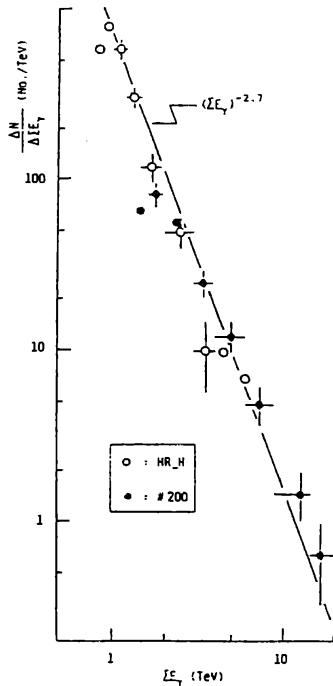


Fig. 6. Differential spectrum of E obtained by the present experiment.

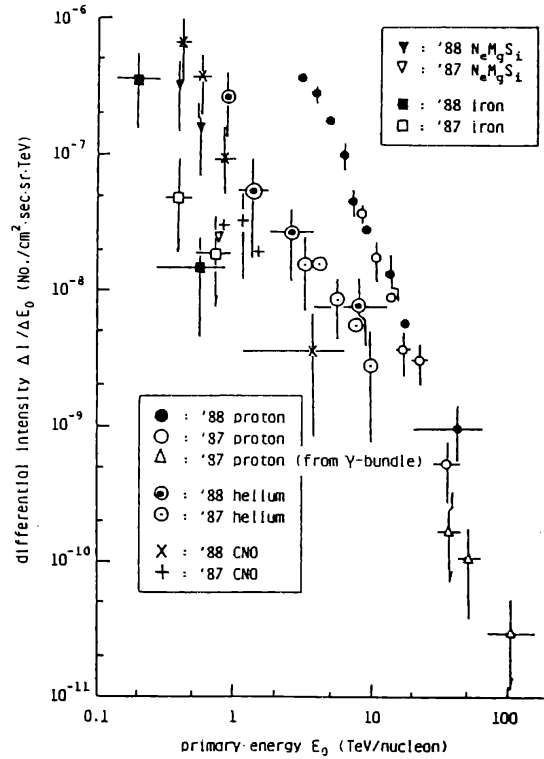


Fig. 7. Differential primary energy spectrum for various kinds of components obtained by '87- and '88-experiments.

by SXF. We can conclude the shower is detected non-biasly down to ~ 0.9 TeV.

Charge of primary particle is determined by three methods, etch-pit calibration, δ -ray counting and spot-darkness measurement with use of CR-39, nuclear emulsion plate (7B-type) and SXF, respectively. Detail of these procedures is presented in ref. 1.

Results and discussions In order to get primary energy spectrum, we have to convert the shower energy ΣE_{γ} into primary energy E_0 , and simultaneously to take into account the detection efficiency depending on the chamber structure. We refer the detail of these calculations in ref. 1,

since we have not enough space to discuss here.

In fig. 7, we present the differential intensity of various components obtained by the present experiment as well as those by '87-experiment.

In fig. 8, we show the differential intensity of proton and helium, where the vertical axis is multiplied by $E_0^{2.7}$ in order to emphasize the change of slope of the spectrum. One finds this result is consistent with those obtained

by other groups⁶, though the excess of helium found by both ours and Burnett et al. (JACEE) is rather remarkable beyond the statistical fluctuation, in comparison with the data obtained by Ryan et al..

In fig. 9, we give the intensity of CNO and iron components, together with the data obtained by other groups. Our results show slightly excess flux in both CNO and iron components in comparison with JACEE data.

Acknowledgements

We are greatly indebted to the staff of balloon division of Institute of Astronautical Science, Sagami-hara, Japan, for successful balloon flight as well as for giving us kind suggestions for construction of our chamber. We also thank the staff of emulsion division of Institute of Cosmic Ray Laboratory, University of Tokyo, for helpful and valuable discussions for this work.

References

1. Y.Kawamura, H.Matsutani, H.Nanjyo, K.Teraoka, K.Toda, M.Ichimura, K.Kirii, K.Kobayashi, Y.Niihori, T.Shibata, K.Shibata, and Y.Yoshizumi; Phys. Rev. 40D, 729(1989).
2. Y.Kawamura et al.; OG 6.1-6, in this volume.
3. Y.Kawamura et al.; OG 10.5-1, in this proceeding.
4. M.Okamoto and T.Shibata; Nucl. Instr. & Methods, A257, (1987)155.
5. T.Fujinaga, M.Ichimura, Y.Niihori, and T.Shibata; Nucl. Instr. & Methods, A276(1989)317.
6. Other group data are cited from following papers.
M.Ryan, J.F.Ormes, and V.K.Balasubrahmanyam; Phys. Rev. Lett. 28, 985(1972);
M.Simon et al.; Astrophys. J. 237, 712(1980);
Burnett et al.; Proceedings of COSPAR'88 (to be published);
E. Nilsson et al. (HEAO-3); in 18th Int. Cosmic Ray Conference, Bangalore, 1983, Conference Papers, vol. 2, p.21.

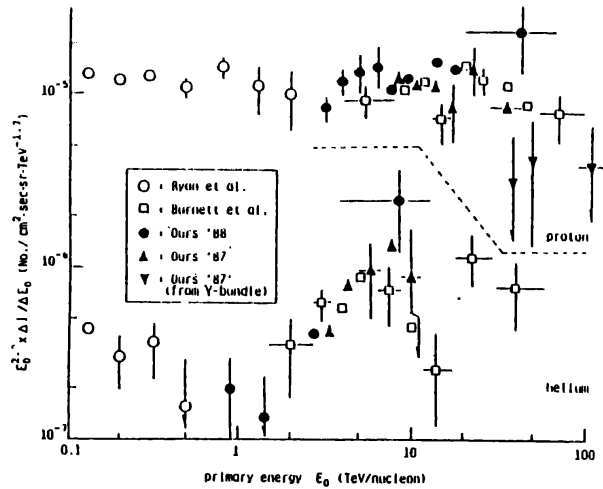


Fig. 8. Primary intensity of proton and helium multiplied by $E_0^{2.7}$.

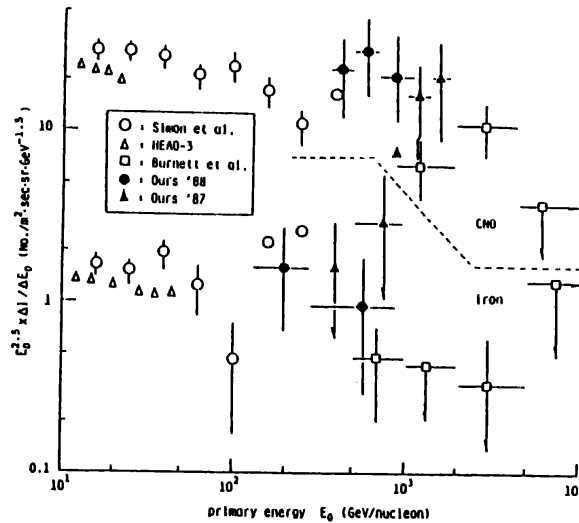


Fig. 9. Primary intensity of CNO and iron components multiplied by $E_0^{2.5}$.